AD-A124 715 FLUTTER PREDICTION IN FORWARD-SWEPT WINGS BY ASSUMED MODES AND STRIP THEORY(U) AIR FORCE INST OF TECH WRIGHT-PATTERSON AFB OH SCHOOL OF ENGI.. W L SHELTON 1/1

UNCLASSIFIED DEC 82 AFIT/GAE/AA/82D-27 F/G 1/1 NL

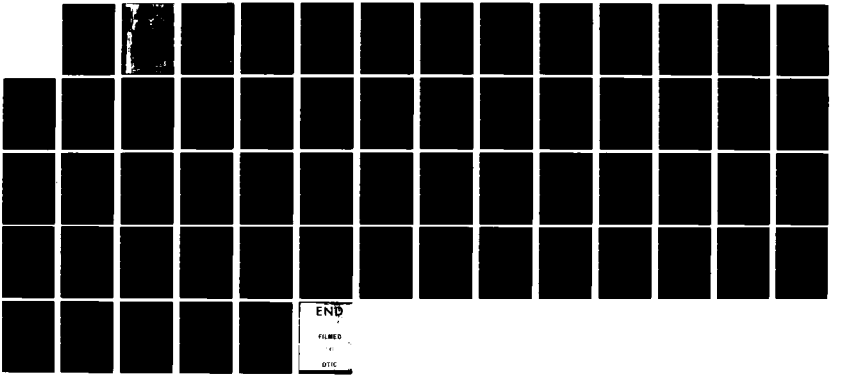

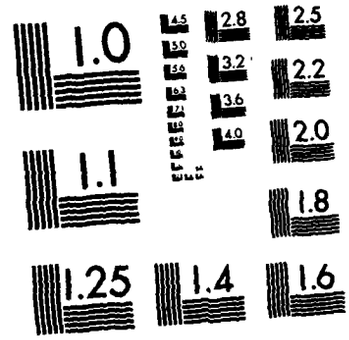

AIR FORCE INSTITUTE OF TECHNOLOGY

AIR UNIVERSITY
UNITED STATES AIR FORCE

FLUTTER PREDICTION IN FORWARD-SWEPT WINGS

BY ASSUMED MODES AND STRIP THEORY

THESIS

AFIT/GAE/AA/82D-27 William L. Shelton, Jr.

SCHOOL OF ENGINEERING

WRIGHT-PATTERSON AIR FORCE BASE, OHIO

AFIT/GAE/AA/82D-27

FLUTTER PREDICTION IN FORWARD-SWEPT WINGS BY ASSUMED MODES AND STRIP THEORY

THESIS

AFIT/GAE/AA/82D-27 William L. Shelton, Jr.

2nd Lt USAF

AFIT/GAE/AA/82D-27

FLUTTER PREDICTION IN FORWARD-SWEPT WINGS BY ASSUMED MODES AND STRIP THEORY

THESIS

Presented to the Faculty of the School of Engineering

of the Air Force Institute of Technology

Air University

in Partial Fufillment of the

Requirements for the Degree of

Master of Science

by

William L. Shelton, Jr., B. S.

2nd Lt USAF

Graduate Aeronautical Engineering

December 1982

Preface

Forward-swept winged aircraft have long been considered because of their aerodynamic advantages. However, until the advent of composite materials, this configuration had been structurally infeasible. Now that the forward-swept wing is practical, the critical failure mode, which past research has found to be divergence, must be explored. This thesis determines flutter speeds, depending on different aerodynamic models and compares them to ascertain the practicality of more advanced aerodynamics.

I would like to thank Dr. Robert Calico, my thesis advisor, for the time, help, and guidance that he gave me. Thanks are due Dr. Franklin Eastep for the aid given me in the aerodynamic modeling and also Dr. Wilhelm Ericksen and Mr. Thomas Noll for their assistance in the actual analysis and computation.

William L. Shelton, Jr.

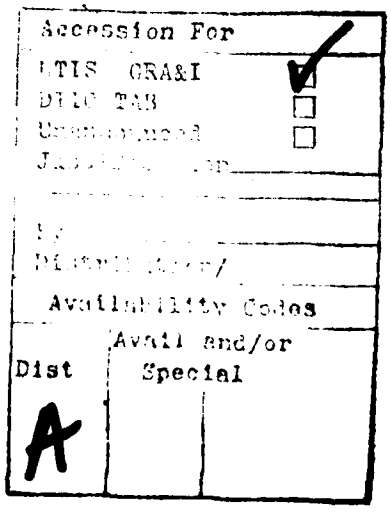

Table of Contents

List of Symbols (Ref 1)

α,θ Torsional angular displacement of entire wing about its elastic axis, in radians.

$\alpha(s),\theta(s)$ Laplacian operator of torsional angular displacement.

b Semi-chord of wing including chord of aileron and tab, in feet.

h,w Bending displacement of wing in direction perpendicular to freestream velocity, positive being down for h and up for w, in feet.

$H(s),W(s)$ Laplacian operator of wing bending displacement.

I_α Moment of inertia per unit span about elastic axis, in slug-feet^2 per foot.

$j=i$ $\sqrt{-1}$

K_α,K_θ Torsional spring constant.

K_h,K_w Bending spring constant.

L Total oscillatory aerodynamic lift acting on wing per unit span, in pounds per foot.

m Mass of wing.

M_y Total oscillatory aerodynamic moment acting on wing about its quarter-chord point per unit span, in pound-feet per foot.

μ Ratio of mass of wing to mass of cylinder of air circumscribed about wing chord, both extending over equal lengths. Note; $\mu=\frac{m}{\pi\rho b^2}$

r_α Radius of gyration of wing about elastic axis as fraction of wing semi-chord.

ρ Density of air, in slugs per cubic foot.

s Laplacian variable for characteristic equations.

U_d Critical divergence speed, in feet per second.

U_f Critical flutter speed, that at which wing system oscillations occur at constant amplitude, in feet per second.

U_∞ Forward speed of aircraft or freestream velocity, in feet per second.

ω_α Uncoupled natural torsional frequency, in radians per second.

ω_h Uncoupled natural bending frequency, in radians per second.

x_α {2(center of gravity)/100}-1-a where center of gravity is given in percent of total chord measured from wing leading edge. Note; $x = \frac{S_\alpha}{mb}$

$\ddot{}$, $\dot{}$ Differentation with respect to time.

List of Figures

Abstract

Flutter speeds for straight wings using quasi-steady and an approximation to unsteady aerodynamics are determined. The same procedure is then followed for both straight and forward-swept wings. The equations of motion for a rigid-body aircraft with the proper aerodynamics are nondimensionalized and the Laplace transforms are taken. After solving the coupled equations simultaneously, various velocities are chosen and the resulting characteristic equations are factored. The roots are then plotted and the flutter or divergence speeds determined.

It was found that flutter speed increased and divergence speed decreased with increasing forward sweep as expected. Also, quasi-steady aerodynamics do not accurately predict flutter and the approximation to unsteady aerodynamics does not accurately predict divergence. It is necessary to combine these two methods in order to obtain a complete analysis of the wing's aeroelastic instabilities.

FLUTTER PREDICTION OF FORWARD-SWEPT WINGS BY ASSUMED MODES AND STRIP THEORY

I. Introduction

Swept wings, both forward and aft, have numerous advantages. Sweeping the wing reduces the velocity component of the freestream that is normal to the leading edge, consequently, the swept wing sees a reduction in drag and weaker shocks in supersonic flight (Ref 11:1-3).

Swept wings drew serious consideration back in 1947 when Collar studied their aeroelastic phenomena at high speeds. Diederich and Budiansky did the first comprehensive treatment of divergence in slender swept wings during 1948. They found that the divergence speed drops rapidly as the amount of forward sweep increases and that wings with a moderate to large amount of aft sweep cannot diverge.

Pros and Cons of Forward-Swept Wings

The forward-swept wing is not a new concept. A four engine jet bomber, the Junkers JU-287, with 15 degrees forward sweep, was built towards the end of World War II. This aircraft actually flew successfully before being damaged on the ground. More recently, the German Hamburger Flugzeugbau HFB-300 Hansa business jet was designed with a swept-forward configuration to create a more spacious fuselage interior. General Dynamics, Grumman and Rockwell International have

all researched the swept-forward wing and, in comparing it with the aft-swept wing, found that it had a lower stall speed, permitting higher manuverability at greater angles of attack and improved slow-speed handling qualities. It exhibited much higher lift to drag ratios in manuvering flight as well as lower trim drag, significantly increasing aircraft range in the supersonic regime. A wing combining these characteristics is one having a lower weight and therefore produces a lower cost aircraft for the same high-performance missions then for an aft-swept wing made of conventional metallic materials.

Until recently, the aerodynamic advantages of forward-swept wings could not be exploited due to its aeroelastic instabilities. When a forward-swept wing is subjected to aerodynamic load, the angle of attack increases. This in turn increases the wing loading and bending, which leads to divergence. To combat this problem of divergence, the wing must be stiffened. However, this solution is prohibitive in that the required stiffening produces a weight penalty which negates any aeroelastic advantages. This problem was studied by Krone (Ref 6:126-127). His report "clearly shows that the detrimental effect of divergence on swept-forward airfoils can be controlled by use of advanced composite materials" (Ref 6:126-127).

Thesis Objectives

This thesis examines the forward-swept wing, using quasi-steady and an approximation to unsteady aerodynamics, to determine the wing's critical flutter speed. These cases are compared and the difference in flutter speed noted. The magnitude of this difference determines whether both types of aerodynamics are used to ascertain the forward-

swept wing's critical flutter speed. Once flutter or divergence speeds are obtained, the zeros of the characteristic equations are traced in an effort to gain some insight into future flutter compensation.

Solution Approach

The solution approach is a straight-forward one. The equations of motion are written and the proper aerodynamics substituted in. Then, using strip theory and assumed modes, the resulting coupled lift and moment equations are applied to the wing of interest. The coupled equations are nondimensionalized, then solved simultaneously through Laplace transforms and matrix techniques. The coefficients of the resulting characteristic equation are functions of velocity only. Varying the velocity generates new characteristic equations, the roots of which are plotted in a root locus technique to determine the wing's critical flutter speed.

II. Theory

Flutter, a dynamic instability, is a self-excited vibration of a body that is moving in a fluid stream. Classically, this is a mechanism involving the coupling of at least two degrees of freedom of the system. These degrees of freedom are stable when uncoupled such that they sustain an oscillating motion. They are critically coupled when there is a phase difference in the oscillatory motion and a time difference between the aerodynamic loads and the system's resulting motion. Flutter occurs at the lowest airspeed and corresponding circular frequency that the system, flying at a prescribed atmospheric density and temperature, exhibits sustained, simple harmonic motion. The forces necessary to produce this motion are simply those present when an elastic structure is deflected from its undeformed state (Ref 2:527).

Divergence differs from flutter in that divergence is a zero frequency or static aeroelastic instability of an airfoil in torsion and twist. This occurs when the torsional stiffness of the airfoil is exceeded by the aerodynamic twisting forces acting upon it (Ref 10:298).

Consequences of Instabilities

These aeroelastic phenomena, when encountered unknowingly, can have drastic consequences. Divergence can shear a wing off an aircraft with little or no warning. Flutter can result in complete structural failure within a matter of seconds or a few oscillations.

One of the more famous and spectacular examples of flutter is the Tacoma Narrows Bridge in the state of Washington. The bridge was constructed between two cliff faces, funneling the air between them. When the wind velocity reached 42 miles per hour, flutter occurred. This concrete and steel structure underwent displacements of approximately 40 feet, behaving as though it were rubber. Finally, on 7 November 1940, the bridge totally destroyed itself after undergoing half an hour of oscillations (Ref 7:66).

Causes of Instabilities

Aeroelastic phenomena in straight wings is dependent only on the twist about the elastic axis. When the wing is swept in either direction, wing bending becomes very important and greatly complicates matters. Flax and Broadbent at the Royal Aircraft Establishment indicate that for swept wings, the rigid body motions are potentially dominating. Flutter coupling will be between the first normal elastic mode and rigid body pitching. In this case, the flutter circular frequency will be lower then the fundamental normal mode frequency. British investigators recommend that, in flutter analysis of swept wings, the first two or three elastic normal modes and two rigid body modes, pitch and translation for symmetric modes and pitch and roll for antisymmetric modes, be used (Refs 3 and 5).

In a forward-swept wing the center of gravity is generally aft of the elastic axis. This produces a nose-up torsional moment about the elastic axis due to the amount of lift produced by the

airfoil at its aerodynamic center. As the wing of Fig. 1 is deflected, notice that line segment AB is level while line segment CB is canted upwards; point C is higher then point B. Therefore segment BC produces a positive increment of lift. This in turn amplifies the torsional moment already existing about the wing's aerodynamic center. An unstabilizing influence, the nose-up twist shifts the center of pressure outboard. The possibility of divergence increases, but the potential for control reversal diminishes. At speeds below what is to be called the critical divergence speed, these increments of lift and twist become smaller and smaller so that an equilibrium condition is attained. However, above this critical speed, the process is decidedly unstable.

Typical Sections

For typical multispar, thick skin structures, it has been found that design stress considerations in the vicinity of the wing root results in a root section so stiff that the wing behaves as a beam clamped perpendicular to its elastic axis (Ref 10:347). Theodorsen and Garrick used representative sections specialized for torsion and bending degrees of freedom (Ref 2:533). The authors suggest that, for purposes of flutter prediction, the typical section can be made to fairly well represent a straight wing of large span by giving this section the geometric and inertial properties of a station that is three-quarters of the way fom the wing's centerline to its tip. This is demonstrated in Fig. 2.

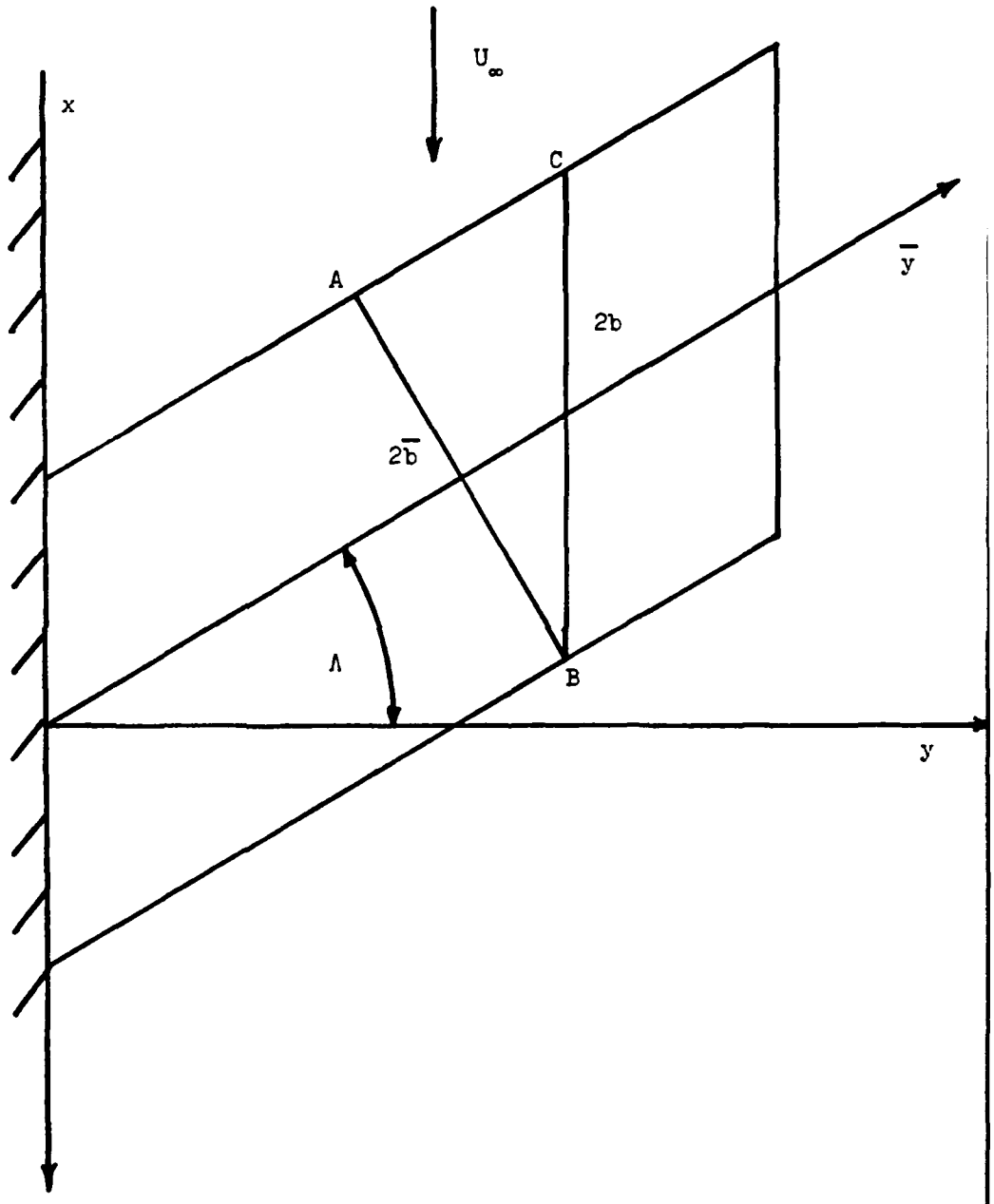

Figure 1. Streamwise and chordwise segments of a forward-swept wing.

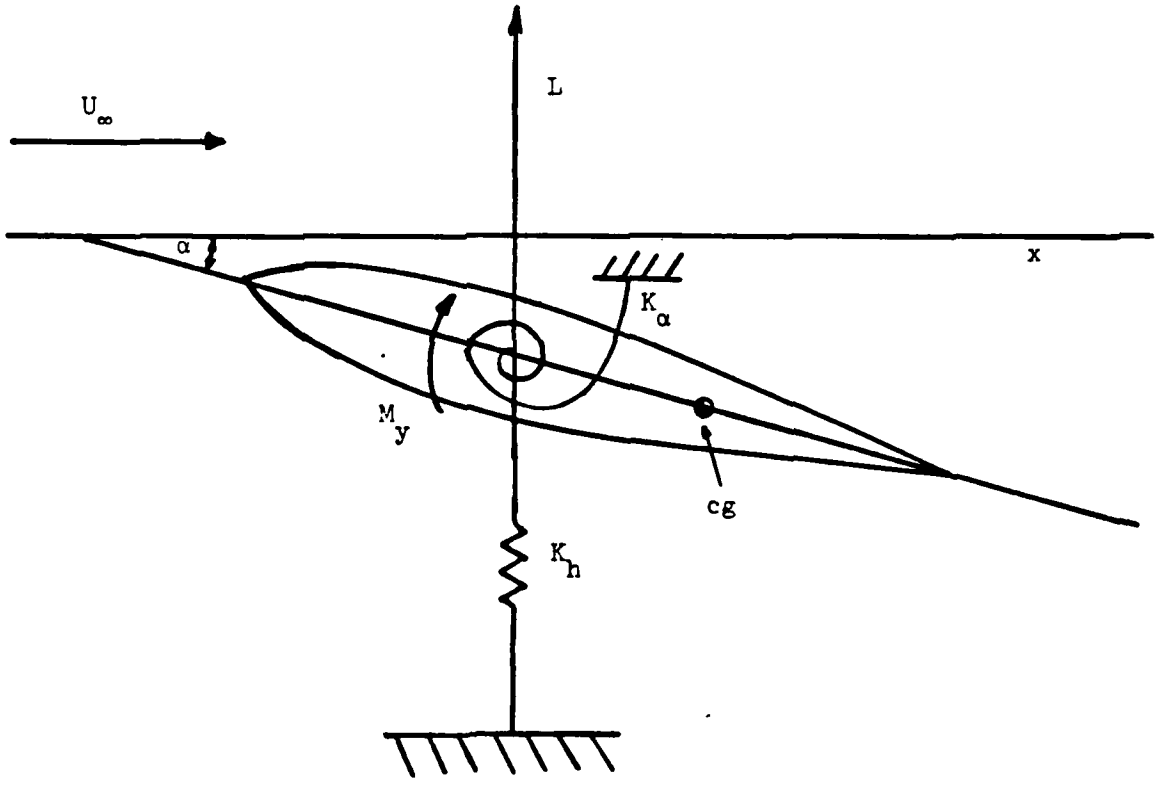

Figure 2. Springs K_α and K_h restrain airfoil from bending and twisting motion in the freestream.

Flutter Prediction

Assumed Modes. In predicting flutter, the continuous aircraft wing is typically modeled using assumed modes. This procedure assumes a solution of the boundary-values associated with a conservative system of the form

$$w(x,t)=\sum_{i=1}^{n} G_i(x)q_i(t) \qquad (1)$$

where $G_i(x)$ is an admissible function, that is one that satisfies only the geometric boundary conditions of the differential equation of the system, and $q_i(t)$ are the generalized coordinates, to be determined, which measure the contribution of each of the admissible functions to the total displacement of the wing surface.

There are two basic guidelines to be followed when selecting functions to be used as assumed modes. They are;

1) Assumed modes should satisfy the geometric boundary conditions and,

2) they should be linearly independent of each other.

It is not absolutely necessary for the assumed modes to satisfy the free-edge natural boundary conditions because the process will tend to satisfy them in the final result. Linear independence requires that it is impossible to express one function as the superposition of the other functions.

Once assumed modes have been selected, the kinetic and potential energies can be determined. It can be shown that the kinetic energy is

$$T(t)=\tfrac{1}{2}\sum_{i=1}^{n}\sum_{j=1}^{n} M_{ij}\dot{q}_i(t)\dot{q}_i(t) \tag{2}$$

and the potential energy is

$$V(t)=\tfrac{1}{2}\sum_{i=1}^{n}\sum_{j=1}^{n} K_{ij}q_i(t)q_i(t) \tag{3}$$

where M_{ij} are the constant symmetric mass coefficients and K_{ij} are the constant symmetric stiffness coefficients, both of which depend on the mass and stiffness distributions, respectively, and the admissible functions, $G_i(x)$. The potential energy generally contains spatial derivatives of $G_i(x)$ that are of orders as half as large as the order of the differential equation of the continuous system that is being considered. Note that the natural boundary conditions are of no concern because they are accounted for automatically in the kinetic and potential energies. Consequently, $G_i(x)$ needs to be an admissible function only.

Lagrange's equations may now be written and are given by

$$\frac{d}{dt}\left[\frac{\partial T}{\partial \dot{q}_r}\right] - \frac{\partial T}{\partial q_r} \quad \frac{\partial V}{\partial q_r} = 0, \; r=1,2,\ldots,n \tag{4}$$

where the q_r represent the non-conservative forces present. Using Eqs. 2 and 3, the equations of motion become

$$\sum_{j=1}^{n} M_{rj}\ddot{q}_j(t) + \sum_{j=1}^{n} K_{rj}q_j(t) = 0, \; r=1,2,\ldots,n \tag{5}$$

which, in matrix form, is

$$|m|\{\ddot{q}(t)\} + |k|\{q(t)\} = \{0\} \tag{6}$$

These linear constant coeficient equations can now be solved for the

$q_i(t)$ and hence, along with the assumed modes $G_i(x)$, form $w(x,t)$ (Ref 8:266-268).

Strip Theory. Strip theory is used to find the approximate solutions to two dimensional theoretical aerodynamic problems. It assumes that the loads of each spanwise station along the wing is dependent only upon the motion of that station at any given time. This theory also assumes that there is no spanwise flow along the wing.

The wing is divided into "strips" and the aerodynamic forces upon each "strip" are calculated. The aerodynamic loads are based on the two dimensional coefficients evaluated at the centerline of each section.

This estimation is well-suited for the evaluation of aerodynamic loads on a straight wing. When this procedure is applied to a wing with sweep, an approximate correction, $\cos\Lambda$, must be applied, where Λ is the quarter-chord sweep angle (Ref 9:17.5-8 - 17.5-9).

Equations of Motion. When a wing is represented by an elastic surface that is thin compared to its span and chord, the equations of motion can be found through the use of influence functions. The wing is also assumed to be rigid in the chordwise direction and is then taken to be straight and to have no structural discontinuities so that the existence of an elastic axis may be assumed. This eliminates the elastic coupling between the integral equations of motion, leaving them only inertially coupled. Elimination of this inertial coupling can occur only if the center of gravity of each chordwise section lies

on the axis (Ref 2:102-105).

It is more convenient to utilize the differential equations for the case described above. These can be derived by setting the system to its equilibrium conditions, then balancing its forces and moments. Fig. 3 illustrates the applied and inertial forces acting on the previously described straight wing. From this, the force per unit length is

$$Z(y,t)=F_z(y,t)+m(y)s(y)\ddot{\theta}(y,t)-m(y)\ddot{w}(y,t) \tag{7}$$

and the torque rate of change, with respect to y, about the elastic axis is

$$T'(y,t)=-t(y,t)+s(y)\{m(y)s(y)\ddot{\theta}(y,t)-m(y)\ddot{w}(y,t)\}+I_{cg}(y)\ddot{\theta}(y,t) \tag{8}$$

as seen from Fig. 4 also. Because this is a thin wing, rotary inertia and shear deformation may be neglected. Therefore, these results may be substituted into

$$\{EIw''(y,t)\}''=Z(y,t) \tag{9}$$

$$\{GJ\theta'(y,t)\}'=T'(y,t) \tag{10}$$

Consequently, the partial differential equations of motion are

$$m(y)\ddot{w}(y,t)-S_y(y)\ddot{\theta}(y,t)+\{EIw''(y,t)\}''=F_z(y,t) \tag{11}$$

$$I_y(y)\ddot{\theta}(y,t)-S_y(y)\ddot{w}(y,t)-\{GJ\theta'(y,t)\}'=t(y,t) \tag{12}$$

where S_y is the static mass moment per unit length about the elastic axis and I_y is the mass moment of inertia about the elastic axis (Ref

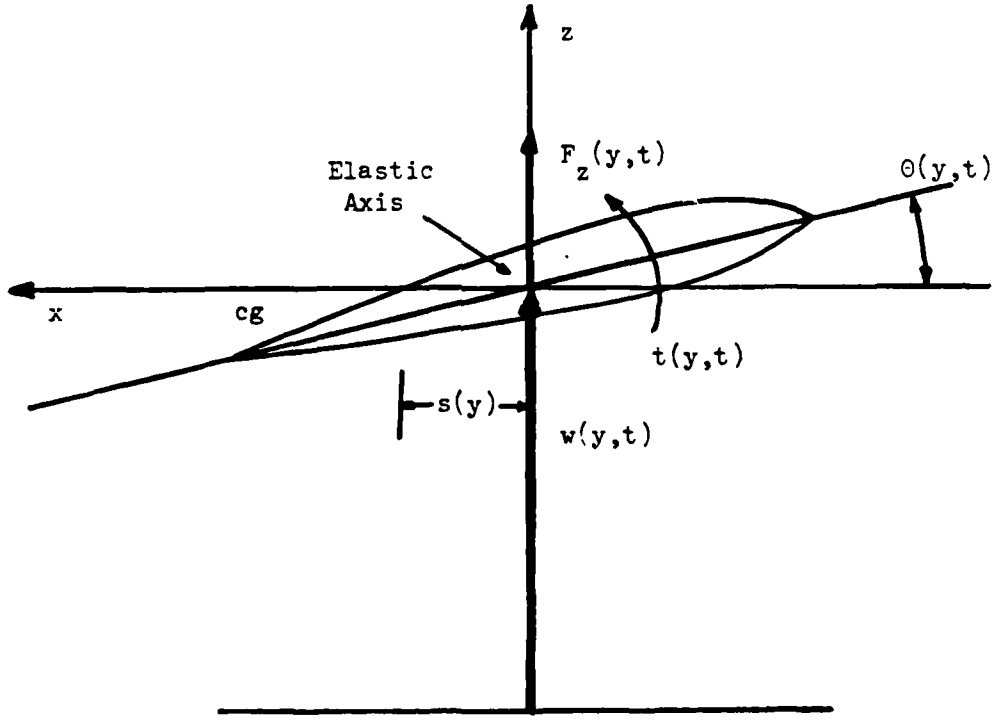

Figure 3. Airplane wing with rigid chordwise segments.

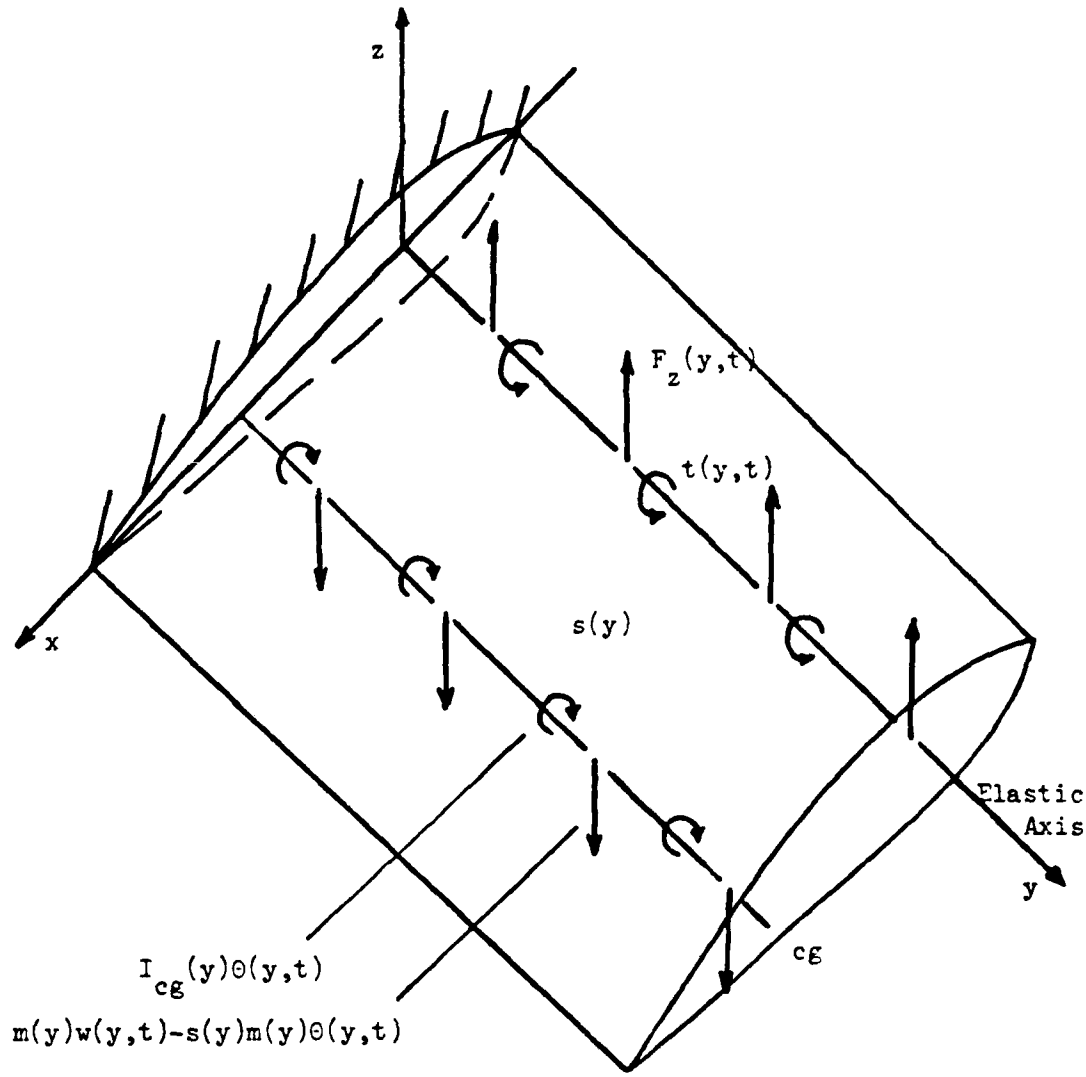

Figure 4. Airplane wing with straight elastic axis.

2:102-106).

Referring to Figs. 5 and 6, Eqs. 10 and 11 can be used to describe a beam under generalized loading. Substituting the aerodynamic loads into the right side, and taking EI, GJ, m, etc. to be constant, produces

$$m\ddot{w}(y,t)-S_y\ddot{\theta}(y,t)+EI\frac{\partial^4}{\partial y^4}w(y,t)=L(y,t) \tag{13}$$

$$I_y\ddot{\theta}(y,t)-S_y\ddot{w}(y,t)-GJ\frac{\partial^2}{\partial y^2}(y,t)=M_y(y,t) \tag{14}$$

where $L(y,t)$ and $M_y(y,t)$ are the aerodynamic lift and moment. These are the equations of motion used in this thesis (Ref 2:546).

Solution Approach. Once the equations of motion are obtained, several substitutions are necessary to put them in a convienent form to use. Notice that there are fourth and second order partial derivatives in the lift and moment equations, respectively. To simplify these partial differential equations, the expression for a beam in bending (Ref 8:209),

$$EI\frac{\partial^4}{\partial y^4}w(y,t)-m\omega_h^2w(y,t)=0 \tag{15}$$

and, in torsion (Ref 8:194-195),

$$GJ\frac{\partial^2}{\partial y^2}\theta(y,t)+I_y\omega_\alpha^2\,\theta(y,t)=0 \tag{16}$$

is used. This yields the simplified the partial differential

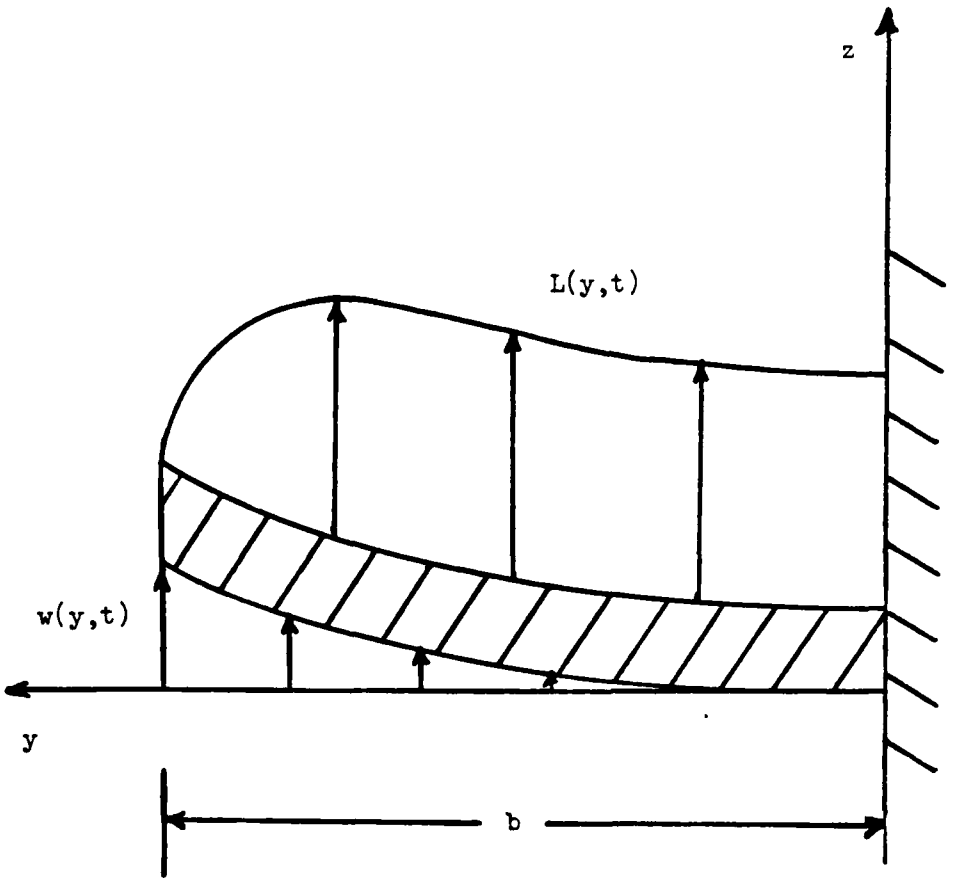

Figure 5. Uniform restrained wing deforming in bending under aerodynamic load, L(y,t).

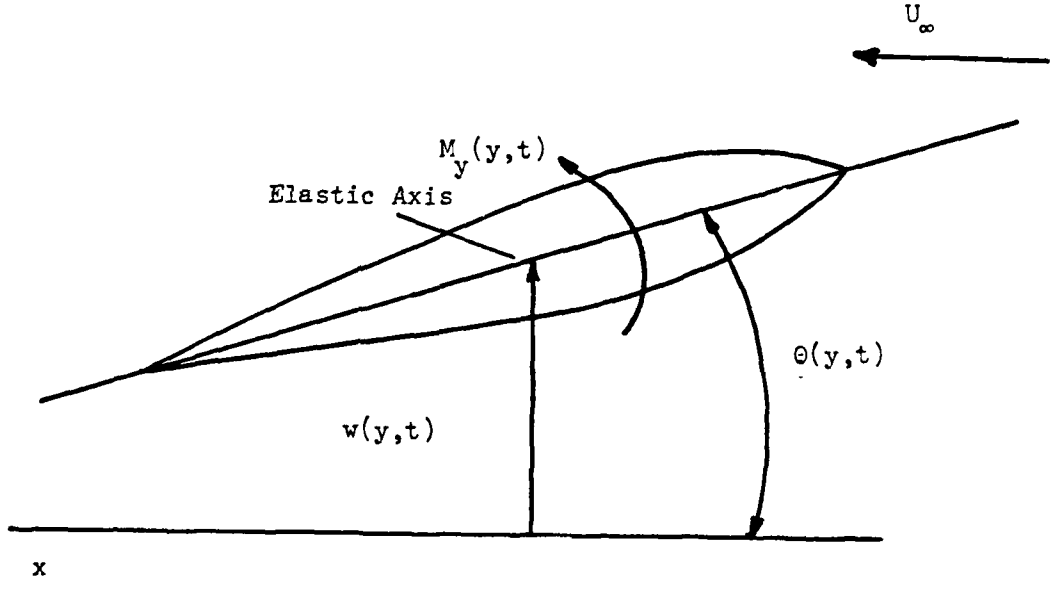

Figure 6. Uniform unrestrained wing deforming in torsion under aerodynamic load, $M_y(y,t)$.

equations of motion, namely

$$m\ddot{w}(y,t)-S_y\ddot{\theta}(y,t)+m\omega_h^2 w(y,t)=L(y,t) \tag{17}$$

and

$$I_y\ddot{\theta}(y,t)-S_y\ddot{w}(y,t)+I_y\omega_\alpha^2\theta(y,t)=M_y(y,t) \tag{18}$$

Using the following expressions for static imbalance, S_y, moment of inertia, I_y, and mass ratio, μ,

$$S_y=mbx_\alpha$$

$$I_y=mb^2r_\alpha^2 \tag{19}$$

$$\mu=\frac{m}{\pi\rho b^2}$$

the equations are nondimensionalized. Then the proper aerodynamics for each case are inserted into the right hand side. When assumed mode methods are used, the bending mode is represented by

$$w(y,t)=C_1\left(\frac{y}{b}\right)^2 w_1(t) \tag{20}$$

and the torsional mode by

$$\theta(y,t)=C_2\sin\frac{\pi}{2}\frac{y}{b}\theta_1(y,t) \tag{21}$$

where C_1 and C_2 are dimensionless amplitudes and $(y/b)^2$ and $\sin\frac{\pi}{2}\frac{y}{b}$ were previously $G_i(x)$ and $w_1(t)$ and $\theta_1(t)$ were $q_i(t)$. The lift and moment equations are then weighted by multiplying them each by

$$C_1\left(\frac{y}{b}\right)^2 \tag{22}$$

and

$$C_2 \sin \frac{\pi}{2} \frac{y}{b} \tag{23}$$

respectively.

Strip theory is then used to evaluate the aerodynamic loading on the right hand side of the equations of motion. The wing is divided into five sections of width 0.2b, where b is the half-span of the wing. Once this is accomplished, the loads on each section are integrated over the section's width and the terms summed, generating the expressions for lift and moment. Each term on the left hand side of the equations is also integrated across the half-span.

Geometric and inertial values that are constants for the wing, straight or swept, are substituted into the weighted, integrated equations of motion. The Laplace transforms of these differential equations are then taken and put in a matrix of the form

$$[A(s)]\{x\}=\{b\} \tag{24}$$

and solved simultaneously by setting the determinant of $[A(s)]$ to zero. The resulting polynomial in s has coefficients that are functions of velocity only. Varying the velocity produces new characteristic equations which,when factored, produce roots for a root locus plot similar to Fig. 7.

Because flutter, by definition, occurs as simple harmonic motion, the critical flutter speed occurs as the root locus crosses

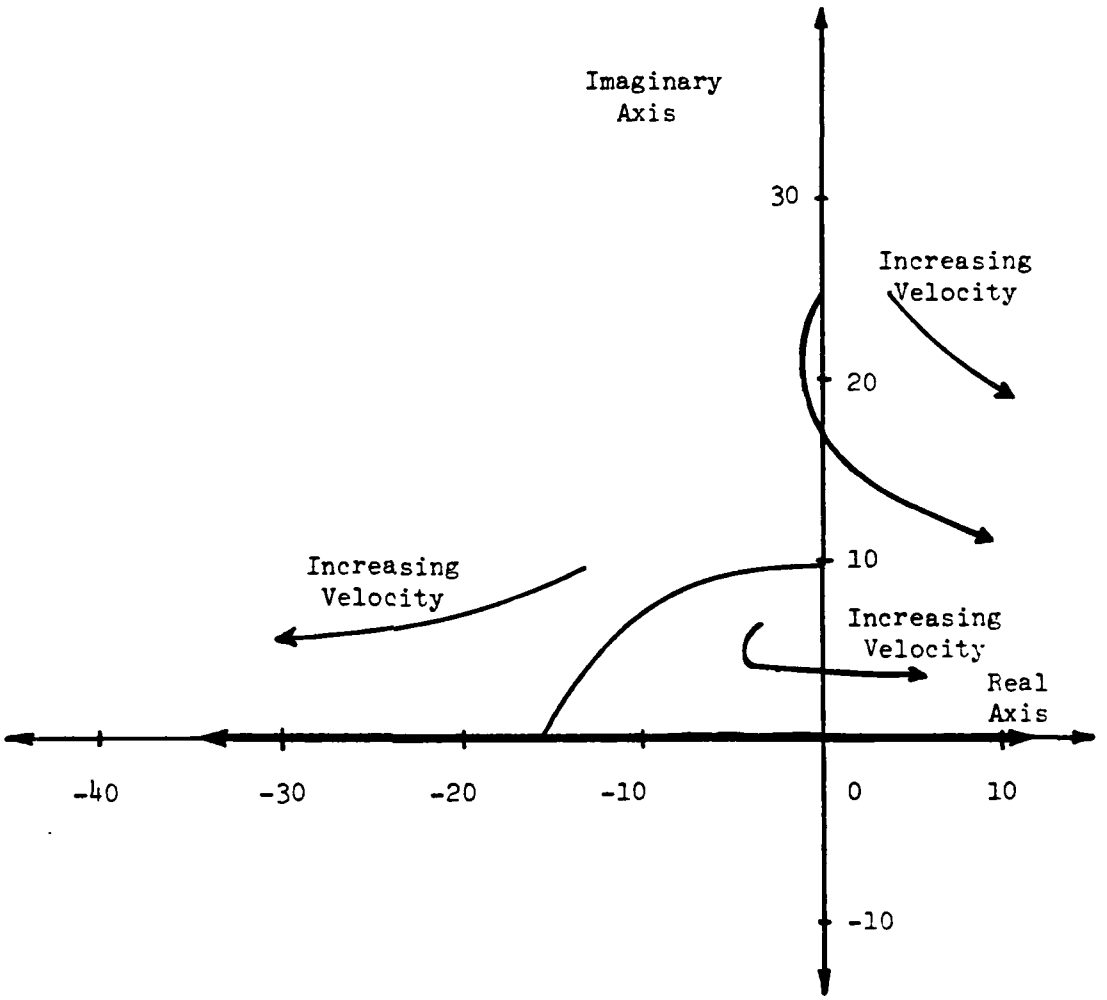

Figure 7. Example of root locus plot to determine flutter and divergence speeds.

the imaginary axis. When the real roots cross the imaginary axis, divergence occurs because this is the zero frequency instability. Details of these calculations are shown in Appendices A through D, depending upon the case of interest.

III. Results

Using the methods described in Appendices A and C, flutter and divergence speeds were found for straight and swept wings using quasi-steady aerodynamics.

The roots of the characteristic equation, resulting from the quasi-steady analysis for a straight wing, are plotted in Fig. 8. From this root locus plot, the flutter speed, U_f, and divergence speed, U_d, can be found. They are the value of velocity at which the high frequency branch crosses the imaginary axis for flutter and the low frequency branch crosses the imaginary axis for divergence. Therefore, from the root locus, it can be seen that U_f is 62.5 ft/sec and U_d is 217.8 ft/sec. Notice the inordinately low flutter speed. Because this is an invalid value, as explained later, root locus plots will not by done for the cases of 15 and 30 degrees of forward sweep. The constant term of the characteristic equation is solved for velocity in the above two cases and the divergence speeds are found to be 157.7 ft/sec for -15 degrees of sweep and 109.2 ft/sec for -30 degrees of sweep.

The exceptionally low flutter speeds are a result of the quasi-steady analysis being inadequate for use at higher reduced frequencies. Guidelines for use of the appropriate aerodynamics with their corresponding frequency ranges can be ascertained through the use of reduced frequency.

The reduced frequency is

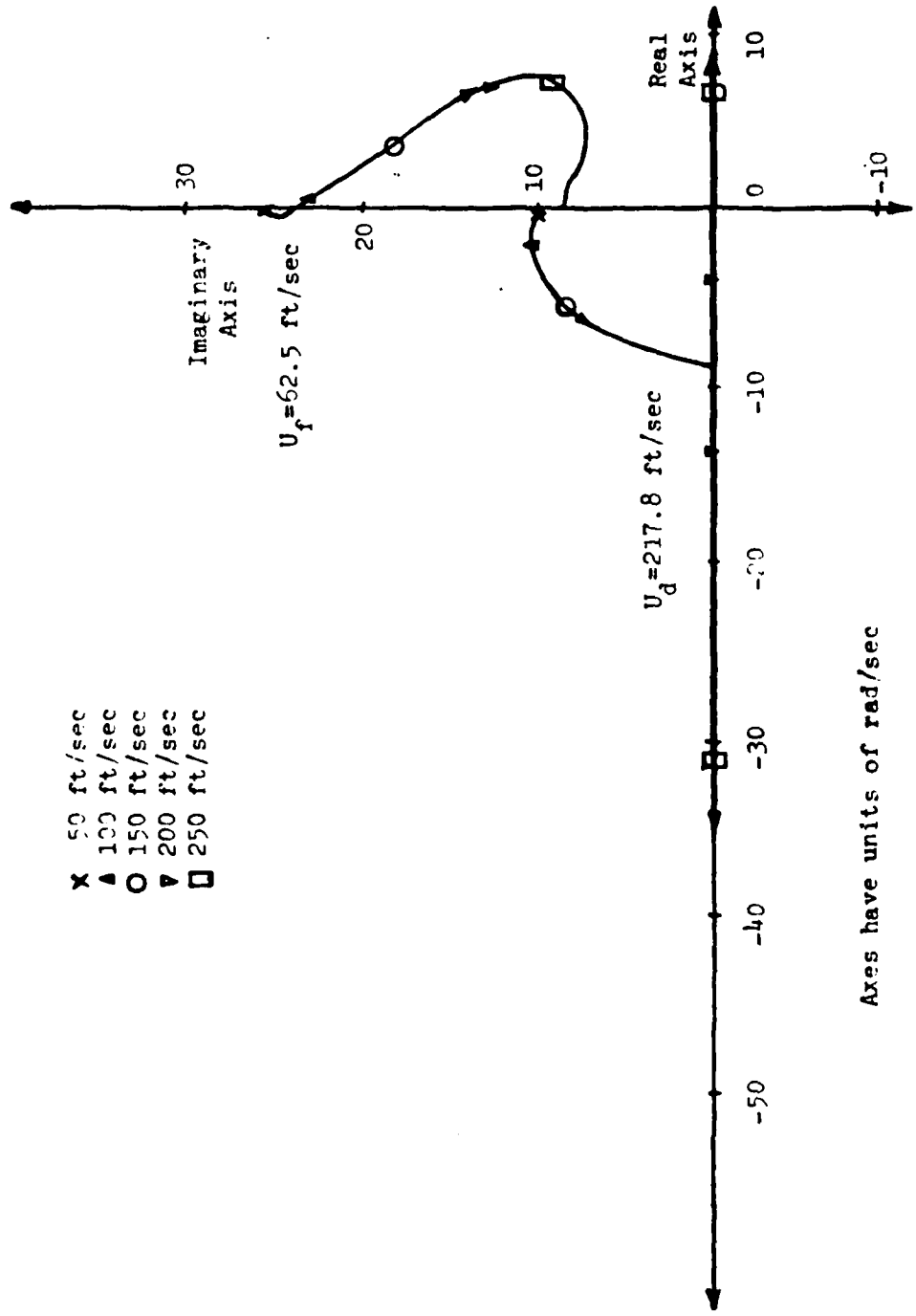

Figure 8. Root locus of flutter analysis of a straight wing with quasi-steady aerodynamics.

$$k=\frac{\omega b}{U} \tag{24}$$

To find the flutter reduced frequency, use the flutter speed and frequency. For quasi-steady aerodynamics, k must be less than 0.2. This reduced frequency restriction is rather strict and is rarely met by typical systems at subsonic speeds. As seen in Table 1, none of the quasi-steady aerodynamic cases are near this value, therefore these are not valid flutter analyses. Because divergence is a zero frequency instability, quasi-steady aerodynamics predict this phenomena quite well. Therefore the divergence speeds are valid values and are plotted in Fig. 9 as a function of sweep angle, Λ.

The methods of Appendices B and D utilize an unsteady aerodynamic model to find the flutter and divergence speeds for a straight wing and ones that are swept forward 15 and 30 degrees. The unsteady aerodynamics utilized an approximation to the complicated Theodorsen functions. This was Jones's approximation and is valid only at higher reduced frequencies. The roots of the characteristic equations for each of these three cases are plotted in Figs. 10, 11 and 12, respectively. From Fig. 10, U_f is shown to be 165.3 ft/sec. For 15 and 30 degrees of forward sweep, U_f is 181.2 and 201.1 ft/sec, respectively. Note that the divergence speed cannot be determined. In the unsteady case, the reduced frequency range changes, as seen in Table 1, and is above the lower limit of 0.2. Consequently, the flutter speeds predicted by the unsteady aerodynamics approximation are good values. The variance of the flutter speed, as predicted by unsteady aerodynamics, is

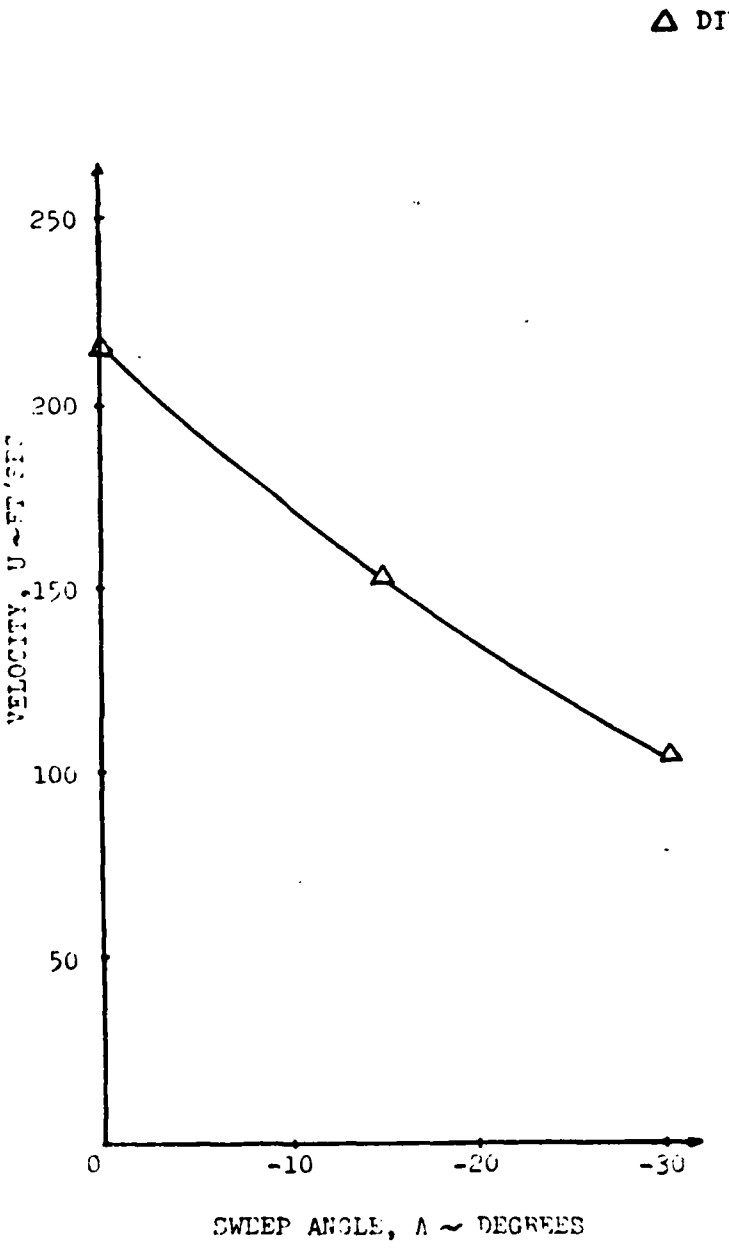

Figure 9. Flutter and divergence speed variations with changes in sweep angle.

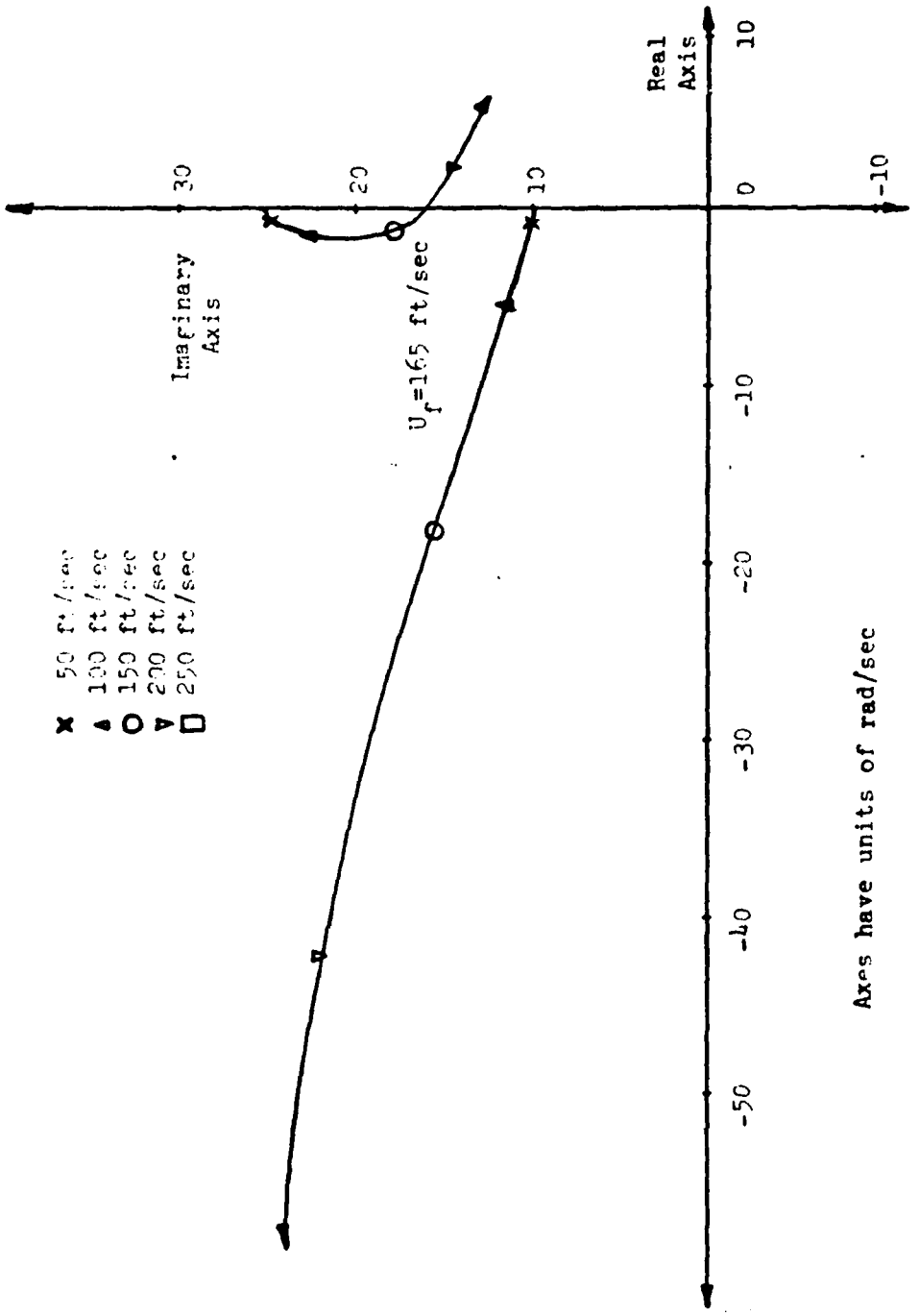

Figure 10. Root locus of flutter analysis of a straight wing with unsteady aerodynamics.

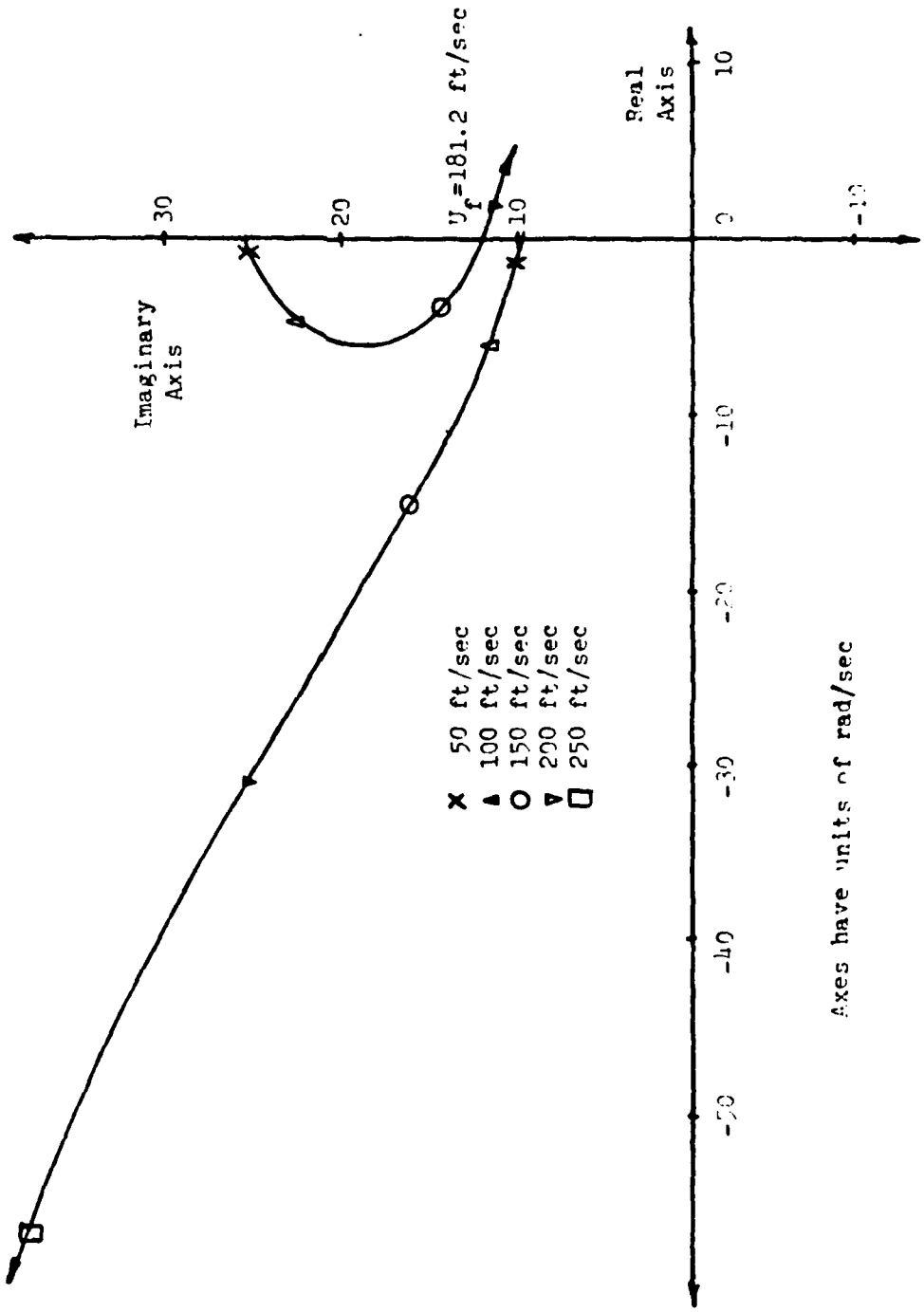

Figure 11. Root locus of flutter analysis of a wing swept forward 15 degrees using unsteady aerodynamics.

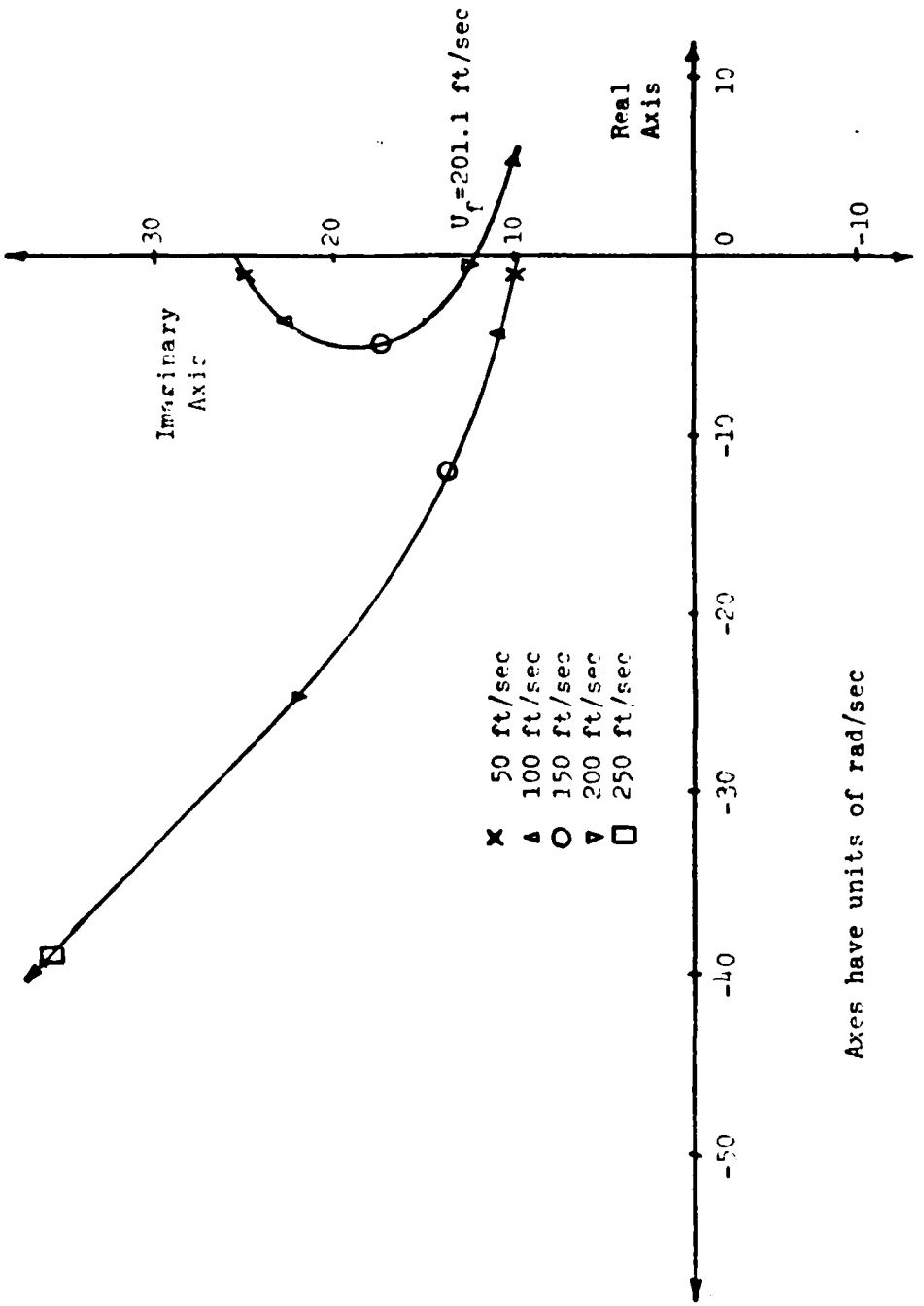

Figure 12. Root locus of flutter analysis of a wing swept forward 30 degrees using unsteady aerodynamics.

Table 1. Ranges of Reduced Frequency

	Reduced frequency, k		
Sweep angle, Λ	0°	-15°	-30°
Quasi-steady aerodynamics	1.11	0.95	0.90
Unsteady aerodynamics	0.29	0.25	0.21

shown in Fig. 15. The same trend in flutter in flutter speed is displayed here as it was in the quasi-steady aerodynamic cases. Unfortunately, the approximation to the unsteady aerodynamics do not do a good job at predicting the critical divergence speed. Again this is due to the discrepancies in the reduced frequency range.

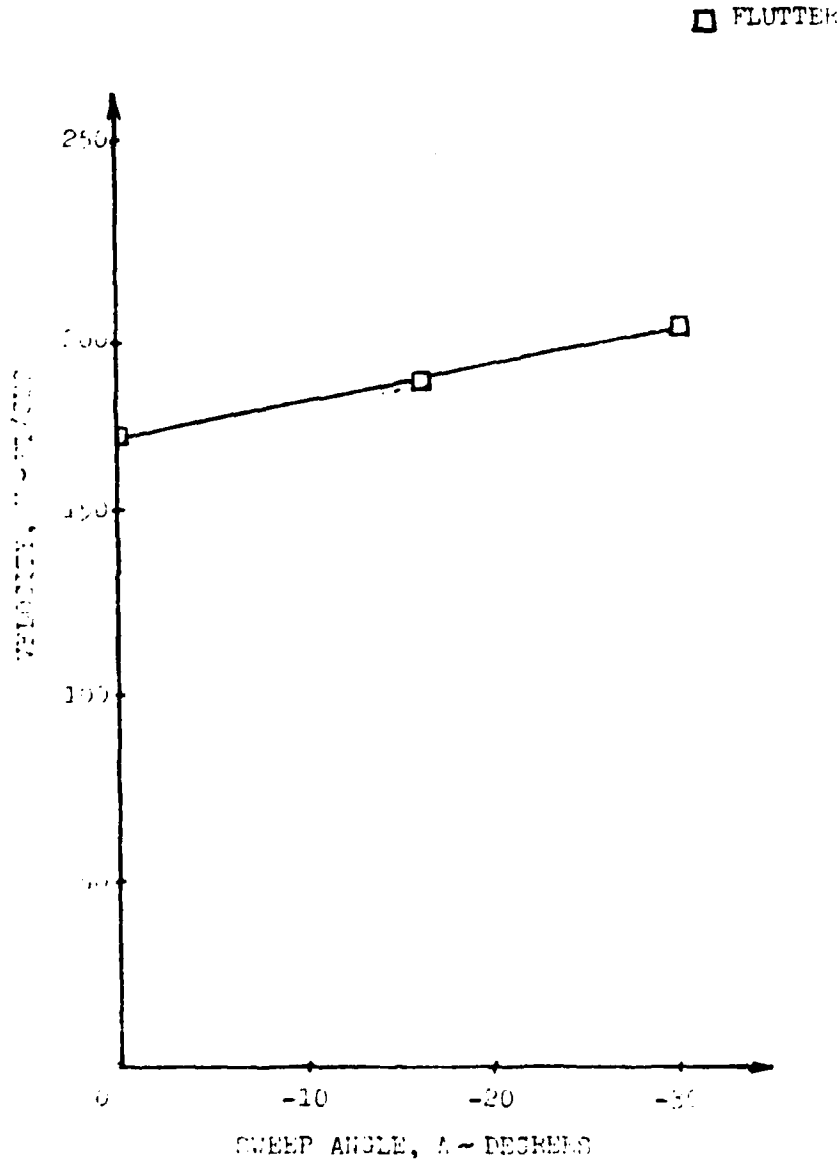

Figure 13. Variance of flutter speed with changes in forward sweep angle.

IV. Conclusions

Flutter analysis, using assumed modes and strip theory, is a straight forward process. To get valid results, however, the proper aerodynamics must be used for each case.

Quasi-steady and the approximation to the unsteady aerodynamics are relatively easy to use and do not require the use of a computer. Once the unsteady aerodynamics are sweep-corrected though, it is impractical to perform the necessary algebraic manipulations by hand. Even though the use of the MAC Symbolic Manipulation System, see Appendix D, reduces this tedious job significantly, it is still highly inefficient. Therefore, unless it is unavoidable, these expressions should not be used.

The two aerodynamic cases examined here are at the opposite ends of the frequency spectrum. This leaves a gap which potentially may be filled by the Pade approximation. This approximation represents the transformed aerodynamic forces as a ratio of polynomials that are a function of the Laplace transform variable s, as did the Jones's approximation. The coefficients of these polynomials are found using a two step least squares process. The generalized aerodynamic forces are obtained from the Pade approximation of sinusoidal forces using doublet-lattice aerodynamics (Ref 4:885-886).

The aeroelastic instability of flutter occurs when at least two degrees of freedom of the system coalesce. Typically, for aft-swept wings, this is between the first bending and first torsion

modes. When looking at forward-swept wings the short period pitching of the aircraft combines with its low frequency mode, producing flutter. The Pade approximation should be compared with the quasi-steady analysis and that of the unsteady approximation to find the theory that yields the most accurate results.

This thesis has laid the groundwork for this comparison and an analysis, such as the one described above for a swept wing, would be a logical follow-on.

Bibliography

1. Air Corps Technical Report 4798, July 1942.

2. Bisplinghoff, Raymond, L. Aeroelasticity, Reading, Massachusetts: Addison-Wesley Publishing Co., Inc., 1955.

3. Broadbent, E. G. "Some Considerations of the Flutter Problems of High Speed Aircraft," Second International Aeronautical Conference, published by Institute of Aeronautical Sciences, Inc., New York, 1947.

4. Eastep, Franklin E. and K. E. Griffin. "Active Control of Forward-Swept Wings with Divergence and Flutter Aeroelastic Instabilities," Journal of Aircraft, Vol. 19, No. 10, October 1982.

5. Flax, A. H. "Aeroelastic Problems at Supersonic Speed," Second International Aeronautical Conference, published by Institute of Aeronautical Sciences, New York, 1949.

6. "Forward-Swept Wing Potential Studied," Aviation Week and Space Technology, Vol. 29, January 1979.

7. Fung, Yuan-chen. An Introduction to the Theory of Aeroelastiscity, New York: John Wiley and Sons, Inc., 1955.

8. Meirovitch, Leonard. Elements of Vibration Analysis, St. Louis: McGraw-Hill Book Co., 1975.

9. NASTRAN Theoretical Manual, Washington, D. C.: Scientific and Technical Information Office, NASA, January 1981.

10. Scanlan, Robert H. Introduction to the Study of Aircraft Vibration and Flutter, New York: The MacMillan Co.,1951.

11. Uhuad, G. C., Capt., USAF. "A Wind Tunnel Test of Half-Span Forward-Swept Wing Model with Variable Canard Location," AFWAL-TM-82-189-FIMM, May 1982.

Appendix A

Flutter analysis of a straight wing using quasi-steady aerodynamics is a straight-forward process. The equations of motion are (Ref 2:546)

$$m\ddot{w}(y,t)-S_\alpha\ddot{\theta}(y,t)+EI\frac{\partial^4}{\partial y^4}w(y,t)=L(y,t) \tag{A1}$$

$$I_\alpha\ddot{\theta}(y,t)-S_\alpha\ddot{w}(y,t)-GJ\frac{\partial^2}{\partial y^2}\theta(y,t)=M_y(y,t) \tag{A2}$$

The equations for a beam in bending and in torsion, respectively, are (Ref 8:209, 194-195)

$$EI\frac{\partial^4}{\partial y^4}w(y,t)-m\omega_h^2w(y,t)=0 \tag{A3}$$

$$GJ\frac{\partial^2}{\partial y^2}\theta(y,t)+I_\alpha\omega_\alpha^2\theta(y,t)=0 \tag{A4}$$

Substituting the expressions for quasi-steady aerodynamic lift and moment (Ref 2:279),

$$L(y,t)=2\pi\rho Ub\{U\theta(y,t)-\dot{w}(y,t)\} \tag{A5}$$

$$M_y(y,t)=L(y,t)b(a+\tfrac{1}{2}) \tag{A6}$$

and Eqs. A3 and A4 into Eqs. A1 and A2, respectively, results in

$$m\ddot{w}-S_\alpha\ddot{\theta}+m\omega_h^2 w=2\pi\rho Ub(U\theta-\dot{w}) \tag{A7}$$

$$I_\alpha\ddot{\theta}-S_\alpha\ddot{w}+I_\alpha\omega_\alpha^2\theta=2\pi\rho Ub^2(a+\tfrac{1}{2})(U\theta-\dot{w}) \tag{A8}$$

To make use of the method of assumed modes, each equation of motion must be weighted by its generalized coordinates. The functions $C_1(\frac{y}{b})^2$ and $C_2\sin\frac{\pi y}{2b}$ were chosen to weight the lift and moment equations, respectively, because the bending of the wing is closely approximated by a parabolic and the twisting by a sinusoidal function.

For similar reasons, the assumed mode shapes of bending and torsion are taken to be

$$w(y,t)=C_1(\frac{y}{b})^2 w_1(t) \tag{A9}$$

$$\theta(y,t)=C_2\sin\frac{\pi y}{2b}\theta_1(t) \tag{A10}$$

When Eqs. A5 and A6 are weighted and mode shapes substituted in, Eqs. A11 and A12 are the results.

$$C_1^2 m(\frac{y}{b})^4 \ddot{w}_1 C_1 C_2 S_\alpha(\frac{y}{b})^2\sin\frac{\pi y}{2b}\ddot{\theta}_1+C_1^2 m\omega_h^2(\frac{y}{b})^4 w_1=$$
$$C_1 2\pi\rho b(\frac{y}{b})^4 U(U\theta-\dot{w}) \tag{A11}$$

$$C_2^2 I_\alpha\sin^2\frac{\pi y}{2b}\ddot{\theta}_1-C_1C_2S_\alpha(\frac{y}{b})^2\sin\frac{\pi y}{2b}\ddot{w}_1+C_2^2 I_\alpha\omega_\alpha^2\sin^2\frac{\pi y}{2b}\theta_1=$$
$$C_2 2\pi\rho Ub^2(a+\tfrac{1}{2})\sin\frac{\pi y}{2b}(U\theta-\dot{w}) \tag{A12}$$

Employing strip theory requires that the right hand sides of

Eqs. A11 and A12 be divided into "strips" and integrated over that strip. Strips of width 0.2b were chosen. The left hand side must also be integrated, but this is done only across the semi-chord, b, and not divided into strips. Once this has been accomplished, Eqs. A11 and A12 are nondimensionalized using the quantities,

$$S_\alpha = mbx_\alpha$$

$$\mu = \frac{m}{\pi \rho b^2} \tag{A13}$$

$$I_\alpha = mb^2 r_\alpha^2$$

Once this has been accomplished, the weighted, integrated equations are

$$0.2\frac{w}{b}_1 - \frac{C}{C_2}_1(0.295)x_\alpha \ddot{\theta}_1 + 0.2\omega_{hb}^2 \frac{w}{b}_1 =$$

$$-\frac{1.257}{\pi}\frac{1}{\mu}\frac{U}{b}\dot{\frac{w}{b}}_1 + \frac{1.851}{\pi}\frac{C_2}{C_1}\frac{1}{\mu}\left(\frac{U}{b}\right)\theta_1 \tag{A14}$$

$$\ddot{\theta}_1 - \frac{C}{C_2}_1(0.589)\frac{x_\alpha}{r_\alpha}\frac{w}{b}_1 + \omega_\alpha^2 \theta_1 =$$

$$\frac{4}{\mu}\frac{(a+\frac{1}{2})}{r_\alpha^2}\left\{0.494\left(\frac{U}{b}\right)^2\theta_1 - \frac{C}{C_2}_1(0.295)\frac{U}{b}\dot{\frac{w}{b}}_1\right\} \tag{A15}$$

These equations must be solved simultaneously and to do so, their Laplace transforms must be taken. It is assumed that the initial conditions are zero so consequently, the transformed equations are

$$\{0.2s^2+\frac{1.257}{\pi}\frac{1}{\mu}\frac{U}{b}s+0.2\omega_h^2\}\frac{w}{b}1(s)$$

$$-\frac{C}{C_1}2\{0.295\,x_\alpha s^2+\frac{1.851}{\pi}\frac{1}{\mu}(\frac{U}{b})^2\}\theta_1(s)=0 \qquad \text{(A16)}$$

$$-\frac{C}{C_2}1\{0.589\,\frac{x_\alpha}{r_\alpha^2}s-\frac{1.18}{\pi}\frac{(a+\frac{1}{2})}{r_\alpha^2}\frac{U}{b}s\}\frac{w}{b}1(s)$$

$$+\{s^2+\omega_\alpha^2-\frac{1.974}{\mu}\frac{(a+\frac{1}{2})}{r_\alpha^2}(\frac{U}{b})^2\}\theta_1(s)=0 \qquad \text{(A17)}$$

For the wing being analysed,

ω_h=10 rad/sec

ω_α=25 rad/sec

x_α=0.1

r_α=0.5

a=-0.2

b=3 ft

μ=20

Using these constants in Eqs. A16 and A17,

$$(s^2+0.033Us+100)\frac{w}{b}1-\frac{C}{C_1}2(0.147s^2+0.016U^2)\theta_1=0 \qquad \text{(A18)}$$

$$-\frac{C}{C_2}1(0.236s^2-0.024Us)\frac{w}{b}1+(s^2+625-0.013U^2)\theta_1=0 \qquad \text{(A19)}$$

which can easily be put into matrix form, the determinant of which will yield the desired characteristic equation:

$$s^4+0.038Us^3+(751.06-0.018U^2)s^2$$

$$+21.561Us+(64746.71-1.367U^2)=0 \qquad \text{(A20)}$$

This equation has coefficients that are functions of velocity only. Varying the velocity produces new characteristic equations and the roots of these are plotted in a root locus.

Appendix B

Flutter analysis of a straight wing utilizing unsteady aerodynamics follows the same basic procedure as that for a straight wing with quasi-steady aerodynamics, the basic difference being the more complex aerodynamic expression. The same wing equations of motion, generalized coordinates, and mode shapes from Appendix A are used. The new aerodynamic expressions are

$$L(y,t)=\pi\rho b^2\{U\dot{\theta}(y,t)-\dot{w}(y,t)-ba\ddot{\theta}(y,t)\}$$
$$+2\pi\rho UbC(k)\{U\theta(y,t)-\dot{w}(y,t)+b(\tfrac{1}{2}-a)\dot{\theta}(y,t)\} \quad \text{(B1)}$$

$$M_y(y,t)=-\pi\rho b^2\{ba\dot{w}(y,t)+Ub(\tfrac{1}{2}-a)\dot{\theta}(y,t)+b^2(\tfrac{1}{8}+a^2)\ddot{\theta}(y,t)\}$$
$$+2\pi\rho Ub^2(a+\tfrac{1}{2})C(k)\{U\theta(y,t)-\dot{w}(y,t)+b(\tfrac{1}{2}-a)\dot{\theta}(y,t)\} \quad \text{(B2)}$$

(Ref 2:272) where C(k) is a Theodorsen function that is dependent on the reduced frequency, k. Therefore, substituting Eqs. B1 and B2 into Eqs. A1 and A2 from Appendix A results in

$$\frac{\ddot{w}}{b} - x_\alpha\ddot{\theta} + \omega_{hb}^2\frac{w}{b} = \frac{1}{\mu}\{\frac{U}{b}\dot{\theta} - \frac{\dot{w}}{b} - a\ddot{\theta}\} + \frac{2}{\mu}\frac{U}{b}C(k)\{\frac{U}{b}\theta - \frac{\dot{w}}{b} + (\tfrac{1}{2}-a)\dot{\theta}\} \quad \text{(B3)}$$

$$r_\alpha^2 - x_\alpha\frac{\ddot{w}}{b} + r_\alpha^2\omega_\alpha^2\theta = -\frac{1}{\mu}\{a\frac{\dot{w}}{b} + \frac{U}{b}(\tfrac{1}{2}-a)\dot{\theta} + (\frac{1}{8}+a^2)\ddot{\theta}\}$$
$$+2\frac{(a+\frac{1}{2})}{\mu}\frac{U}{b}C(k)\{\frac{U}{b}\theta - \frac{\dot{w}}{b} + (\tfrac{1}{2}-a)\dot{\theta}\} \quad \text{(B4)}$$

Because Theodorsen functions are, in general, very complicated, Jones's approximation

$$C(s)= \frac{.5s^2+ 0.843Us + 0.014U^2}{9s^2+ 1.037Us + 0.014U^2} \tag{B5}$$

(Ref 2) will be utilized instead.

Following the same procedure outlined in Appendix A, the weighted, integrated equations of motion are

$$0.2\frac{w}{b} - \frac{C_2}{C_1}\, 0.0295x_\alpha \ddot{\theta}_1 + 0.2\omega_h^2 \frac{w}{b}1 = \frac{C_2}{C_1}\, 0.295\, \frac{1}{\mu}\, \frac{U}{b}\dot{\theta}_1 - 0.2\frac{w}{b}1$$

$$-\frac{C_2}{C_1}\, 0.295\, \frac{a}{\mu}\, \ddot{\theta}_1 + \frac{C_2}{C_1}\, 0.598\, \frac{1}{\mu}\left(\frac{U^2}{b}\right)C(s) - \frac{0.4}{\mu}\, \frac{U}{b}C(s)\dot{\frac{w}{b}}1$$

$$+ \frac{C_2}{C_1}\, 0.598\, \frac{U}{b}\, (\tfrac{1}{2}-a)C(s)\dot{\theta}_1 \tag{B6}$$

$$0.5r_\alpha^2\ddot{\theta}_1 - \frac{C_1}{C_2}\, 0.295x_\alpha \dot{\frac{w}{b}}1 + 0.5r_\alpha^2\omega_\alpha^2\theta_1 = -\frac{C_1}{C_2}\, 0.295\, \frac{a}{\mu}\, \frac{w}{b}1$$

$$-0.5\, \frac{U}{b}\, \frac{(\frac{1}{2}-a)}{\mu}\, \dot{\theta}_1 - 0.5\frac{(1/8+a^2)}{\mu}\ddot{\theta}_1 + \left(\frac{U}{b}\right)2\frac{(a+\frac{1}{2})}{\mu}C(s)\theta_1$$

$$-\frac{C_1}{C_2}\, 0.591\frac{(a+\frac{1}{2})}{\mu}\, \frac{U}{b}\, C(s)\, \dot{\frac{w}{b}}1 + \frac{(\frac{1}{2}-a^2)}{\mu}\, \frac{U}{b}\, C(s)\, \dot{\theta}_1 \tag{B7}$$

Transforming Eqs. B6 and B7 and using the constant values of Appendix A, yields,

$$\{0.4s^2+0.0067UC(s)s+20\}\frac{w}{b}1$$

$$-\frac{C_2}{C_1}\{0.032s^2+(0.005+0.0069C(s))Us-0.0033U^2C(s)\}\theta_1=0 \tag{B8}$$

$$-\frac{C_1}{C_2}\{0.032s^2+(0.0058-0.0035C(s)s\}\frac{w}{b}1$$

$$+\{0.129s^2+(0.0058-0.0035C(s))Us$$

$$+(78.125-0.0017U^2C(s))\}\theta_1=0 \tag{B9}$$

and solving them simultaneously produces Eq. B10 which is the characteristic equation of the sy.tem:

$$s^6+0.156Us^5+(734.2-0.0031U^2)s^4+(98.75-0.00132U^2)Us^3$$
$$+(60385+2.62U^2-0.000625U^4)s+(6953-0.089U^2)Us$$
$$+(92.07U^2-0.007U^4)=0 \qquad \text{(B10)}$$

Again, Eq. B10 has coefficients that are functions of velocity only. The results of varying the velocity are plotted in a root locus.

Appendix C

Flutter analysis of a swept wing does not differ greatly from that of a straight one. The major difference occurs in the definition of the variables that are dependent upon the spanwise axis. The variables in question are the semi-chord, b, and the mass ratio, μ. They are defined as

$$\bar{b}=\frac{b}{\cos\Lambda} \tag{C1}$$

$$\bar{\mu}=\frac{m}{\pi\rho U\bar{b}^2} \tag{C2}$$

where Λ is the sweep angle, positive being aft. The redefinition of the semi-chord, b, also affects the mode shapes:

$$w=C_1(\frac{\bar{y}}{\bar{b}})^2 w_1 \tag{C3}$$

$$\theta=C_2\sin\frac{\pi}{2}\frac{\bar{y}}{\bar{b}}\theta_1 \tag{C4}$$

The quasi-steady aerodynamic expressions for lift and moment are

$$\begin{aligned}\bar{L}(\bar{y},t)=&\pi\rho\bar{b}^2\{U\dot{\bar{\theta}}\cos\Lambda+U\dot{\sigma}\sin\Lambda-U\bar{b}a\dot{\tau}\sin\Lambda\}\\&+2\pi\rho\bar{b}U\cos\Lambda\{-\dot{w}+U\bar{\theta}\cos\Lambda+U\sigma\sin\Lambda\\&+\bar{b}(\tfrac{1}{2}-a)(\dot{\bar{\theta}}+U\tau\sin\Lambda)\}\end{aligned} \tag{C5}$$

$$M_y(\bar{y},t)=-\pi\rho\bar{b}^3\{U(\tfrac{1}{2}-a)\dot{\bar{\theta}}\cos\Lambda+\tfrac{1}{2}U^2\tau\cos\Lambda\sin\Lambda$$
$$-Ua\dot{\sigma}\sin\Lambda+\bar{b}(\tfrac{1}{8}+a^2)\dot{U\tau}\sin\Lambda\}$$
$$+2\pi\rho\bar{b}^2U\cos\Lambda(\tfrac{1}{2}+a)\{-\dot{w}+U\bar{\theta}\cos\Lambda$$
$$+U\sigma\sin\Lambda+\bar{b}(\tfrac{1}{2}-a)(\dot{\bar{\theta}}+U\tau\sin\Lambda)\} \qquad (C6)$$

where $\sigma=\frac{-\partial w}{\partial\bar{y}}$ and $\tau=\frac{\partial\bar{\theta}}{\partial\bar{y}}$.

Eqs. C5 and C6 are the unsteady aerodynamic expressions that are simplified by the quasi-steady assumptions, namely small disturbances thereby eliminating the accleration terms and C(k) is one (Ref 2:398).

Because divergence is a zero frequency aeroelastic instability, only the constant term of the characteristic equation, which has been greatly complicated by the sweep correction, is of importance. This term of the weighted, integrated, transformed equation is set to 0:

$$U^2(0.0007\sin2\Lambda\cos^2\Lambda-0.99\sin^2 2\Lambda+0.4\sin2\Lambda-0.3\cos\Lambda)$$
$$+U(0.0007\sin2\Lambda)$$
$$+(-0.0002\sin^2 2\Lambda-0.1\sin\Lambda-2.19\sin2\Lambda+15625)=0 \qquad (C7)$$

Selecting Λ to be either -15 or -30 degrees and solving for U will give the divergence speed for that case.

Appendix D

This calculation was greatly complicated by the addition of the sweep-corrected unsteady aerodynamic terms. The new expressions for lift and moment, respectively, are

$$\bar{L}(\bar{y},t)=\rho\bar{b}^2\{-\dot{w}+U\dot{\bar{\theta}}\cos\Lambda+U\dot{\sigma}\sin\Lambda-\bar{b}a\ddot{\bar{\theta}}-\bar{b}aU\dot{\tau}\sin\Lambda\}$$
$$+2\pi\rho\bar{b}U\cos\Lambda C(k)\{-\dot{w}+U\bar{\theta}\cos\Lambda+U\sigma\sin\Lambda+\bar{b}(\tfrac{1}{2}-a)\{\dot{\bar{\theta}}+U\tau\sin\Lambda\}\} \quad (D1)$$

$$M_y(\bar{y},t)=-\pi\rho\bar{b}^3\{U(\tfrac{1}{2}-a)\dot{\bar{\theta}}\cos\Lambda+\tfrac{1}{2}U^2\tau\sin\Lambda\cos\Lambda+aU\dot{\sigma}\sin\Lambda+\bar{b}(\frac{1}{8}+a^2)$$
$$\cdot\{\ddot{\bar{\theta}}+U\dot{\tau}\sin\Lambda\}\}+2\pi\rho\bar{b}^2U\cos\Lambda(\tfrac{1}{2}+a)C(k)\{-\dot{w}+U\bar{\theta}\cos\Lambda+U\sigma\sin\Lambda\bar{b}$$
$$\cdot(\tfrac{1}{2}-a)\{\dot{\bar{\theta}}+U\tau\sin\Lambda\}\} \quad (D2)$$

where

$$\sigma=-\frac{\partial w}{\partial\bar{y}}$$
$$\tau=\frac{\partial\bar{\theta}}{\partial\bar{y}} \quad (D3)$$
$$\bar{\theta}=\frac{\theta}{\cos\Lambda}$$
$$\bar{y}=\frac{y}{\cos\Lambda}$$

(Ref 2:398).

Following the procedure of Appendix B, the nondimensionalized equations for lift and moment are

$$\frac{L}{m\bar{b}} = \frac{1}{\mu\bar{b}}\{-\ddot{w}+U\ddot{\theta}\cos\Lambda+U\dot{\sigma}\sin\Lambda-\bar{b}a\ddot{\theta}-\bar{b}aU\dot{\tau}\sin\Lambda\}$$

$$+\frac{2}{\mu\bar{b}^2}U\cos\Lambda C(k)\{-\dot{w}+U\bar{\theta}\cos\Lambda+U\sigma\sin\Lambda+\bar{b}(\tfrac{1}{2}-a)\{\dot{\bar{\theta}}+U\tau\sin\Lambda\}\} \qquad (D4)$$

$$\frac{M_y}{m\bar{b}^2} = \frac{-1}{\mu\bar{b}}\{U(\tfrac{1}{2}-a)\dot{\bar{\theta}}\cos\Lambda+\tfrac{1}{2}U^2\tau\sin\Lambda\cos\Lambda+aw-Ua\dot{\sigma}\sin\Lambda+b(\tfrac{1}{8}+a^2)$$

$$\cdot\{\ddot{\bar{\theta}}+U\dot{\tau}\sin\Lambda\}\}+\frac{2}{\mu\bar{b}}U\cos\Lambda(\tfrac{1}{2}+a)C(k)\{-w+U\bar{\theta}\cos\Lambda+U\sigma\sin\Lambda$$

$$+\bar{b}(\tfrac{1}{2}-a)\{\dot{\bar{\theta}}+U\tau\sin\Lambda\}\} \qquad (D5)$$

The equations are weighted and integrated using the same constants and equations of motion as before, then taking their Laplace transforms, resulting in

$$C_1^2\{1.05s^2+(0.0355C(s)-0.0415\tan\Lambda)Us$$

$$+(100-0.014\sin2\Lambda C(s))U\}\frac{w_1}{\bar{b}}(s)$$

$$-C_1C_3\{(0.11+\frac{0.011}{\cos\Lambda})s^2+(0.018+0.023C(s)+0.006\tan\Lambda)Us$$

$$+(0.0033\cos^2\Lambda+0.007)U^2C(s)+0.0029U\sin2\Lambda\}\theta_1(s)=0 \qquad (D6)$$

$$-C_1C_3\{(0.107-\frac{0.051}{\cos\Lambda})s^2-(0.023\sin\Lambda+0.01C(s))Us$$

$$-(0.0114\sin2\Lambda C(s))\}\frac{w_1}{\bar{b}}(s)$$

$$+C_3^2\{(0.25+\frac{0.008}{\cos^2\Lambda})s^2+(0.0116-0.055\tan\Lambda-0.007C(s))Us$$

$$+(156.25+0.0112\sin2\Lambda U^2-0.0034U^2\cos^2\Lambda C(s)$$

$$-0.0012\sin2\Lambda C(s)\}\theta_1(s)=0 \qquad (D7)$$

where C(k) is the Theordorsen function that is approximated by Eq. B5.

Solving these complicated expressions by hand would be very difficult, if not impossible. Therefore, this was accomplished by using the MAC Symbolic Manipulation Syatem (MACSYMA) that was developed by the Massachusetts Institute of Technology Math Lab. This system is an interpeted computer language for algebraic manipulations.

When Eqs. D6 and D7 are solved using MACSYMA, the expression is quite long and complicated and will not be shown here. This equation is a function of sweep argle and velocity, which, when the velocity is varied for angles of 15 and 30 degrees of sweep, produces characteristic equations. The roots of these are plotted on a root locus.

Vita

William L. Shelton, Jr. was born 10 April 1959 in Plattsburgh, New York. After living overseas for two years, he moved to Rockville, Maryland. He graduated from Robert E. Peary High School in the top five percent of his class in 1977. He then attended the Massachusetts Institute of Technology in Cambridge, Massachusetts from which he received the degree of Bachlor of Science in Aeronautics and Astronautics in June 1981. Upon graduation, he was commissioned into the United States Air Force through the Reserve Officers Training Corps (ROTC) program. In June 1981 he entered the School of Engineering, Air Force Institute of Technology, to pursue a Master of Science degree in Aeronautical Engineering.

Permanent Address: 5015 McCall Street

Rockville, MD 20853

UNCLASSIFIED

SECURITY CLASSIFICATION OF THIS PAGE *(When Data Entered)*

REPORT DOCUMENTATION PAGE

READ INSTRUCTIONS BEFORE COMPLETING FORM

1. REPORT NUMBER: AFIT/GAE/AA/82D-27	2. GOVT ACCESSION NO.: AD-A124 715
3. RECIPIENT'S CATALOG NUMBER:	
4. TITLE *(and Subtitle)*: FLUTTER PREDICTION IN FORWARD-SWEPT WINGS BY ASSUMED MODES AND STRIP THEORY	5. TYPE OF REPORT & PERIOD COVERED: MS Thesis
	6. PERFORMING ORG. REPORT NUMBER:
7. AUTHOR(s): William L. Shelton, Jr.	8. CONTRACT OR GRANT NUMBER(s):
9. PERFORMING ORGANIZATION NAME AND ADDRESS: Air Force Institute Of Technology, Wright-Patterson AFB, Ohio 45433	10. PROGRAM ELEMENT, PROJECT, TASK AREA & WORK UNIT NUMBERS:
11. CONTROLLING OFFICE NAME AND ADDRESS:	12. REPORT DATE: December, 1982
	13. NUMBER OF PAGES: 57
14. MONITORING AGENCY NAME & ADDRESS *(if different from Controlling Office)*:	15. SECURITY CLASS. *(of this report)*: Unclassified
	15a. DECLASSIFICATION/DOWNGRADING SCHEDULE:

16. DISTRIBUTION STATEMENT *(of this Report)*

Approved for public release; distribution unlimited

17. DISTRIBUTION STATEMENT *(of the abstract entered in Block 20, if different from Report)*

18. SUPPLEMENTARY NOTES

Approved for public release: IAW AFR 190-17.

LYNN E. WOLAVER
Dean for Research and Professional Development
Air Force Institute of Technology (ATC)
Wright-Patterson AFB OH 45433

19 JAN 1983

19. KEY WORDS *(Continue on reverse side if necessary and identify by block number)*

Flutter
Divergence
Assumed modes
Strip theory
Root locus
Forward-swept wing

20. ABSTRACT *(Continue on reverse side if necessary and identify by block number)*

Flutter speeds for straight wings using quasi-steady and an approximation to unsteady aerodynamics are determined. The same procedure is then followed for both straight and forward-swept wings. The equations of motion for a rigid-body aircraft with the proper aerodynamics are nondimensionalized and the Laplace transforms are taken. After solving the coupled equations simultaneously, various velocities are chosen and the resulting characteristic equations are factored.

DD FORM 1 JAN 73 1473 EDITION OF 1 NOV 65 IS OBSOLETE

UNCLASSIFIED

SECURITY CLASSIFICATION OF THIS PAGE *(When Data Entered)*

The roots are then plotted and the flutter or divergence speeds determined.

It was found that flutter speed increased and divergence speed decreased with increasing forward sweep as expected. Also, quasi-steady aerodynamics do not accurately predict flutter and the approximation to unsteady aerodynamics does not accurately predict divergence. It is necessary to combine these two methods in order to obtain a complete analysis of the wing's aeroelastic instabilities.

END

FILMED

3-83

DTIC